

## **An investigation of using hump in the Cherenkov photon lateral distribution for Gamma-Hadron separation**

Gohar Rastegarzadeh · Sahar Khoshabadi

Department of Physics, Semnan University , University Sq, Pardis No 1, P.O. Box 35195- 363, Semnan, Iran

**Abstract.** Simulation of gamma and hadron showers in the energy range 100GeV-25TeV has been carried out. For a big ideal Cherenkov light array, characteristics of lateral distribution of Cherenkov photon density have been studied. Results from this ideal detector are compared with those simulated for a real TUNKA- like array to investigate experimental potential of using existence of a hump in lateral distribution of Cherenkov photon density for gamma-hadron separation. It is shown that by using this technique the proton rejection efficiency of %63 can be achieved in typical TUNKA-like arrays.

*Keywords:* Cherenkov array, Lateral distribution, hump,  $\gamma$ -ray astronomy

## **1 Introduction**

In recent years, the search for gamma Ray sources has become one of the main concerns for astrophysics, and measuring atmospheric Cherenkov radiation is presently the most effective way to detect These sources [1].

The development of ground-based Imaging Atmospheric Cherenkov Telescopes (IACTs) allowed the detection of gamma ray initiated showers in the Very High Energy domain [2]. These instruments image Cherenkov light emitted by  $\gamma$ -ray induced particle cascades in the atmosphere. Background from the much more numerous cosmic-ray cascades is efficiently reduced by considering the shape of the shower image; and the capability to reduce this background is one of the key aspects that determines the sensitivity of a IACT [3]. In the recent years IACTs opened a previously inaccessible window for the study of astrophysical sources of  $\gamma$  radiation in the VHE regime. The detection of more than 50 galactic VHE  $\gamma$ -ray emitters during the galactic plane scan which was performed by the H.E.S.S.( The High Energy Stereoscopic System) collaboration between 2004 and 2007 decupled the number of known VHE  $\gamma$ -ray sources and hence established a new field in astronomy [3]. Still, for the existing instruments, increased background reduction can improve the sensitivity considerably .

At present, the CTA(Cherenkov Telescope Array) has a large discovery potential in key areas of astronomy, astrophysics and fundamental physics research. These include the study of the origin of cosmic rays and their impact on the constituents of the universe through the investigation of galactic particle accelerators, the exploration of the nature and the examination of a variety of black hole particle accelerators. CTA still has contribution to the study of the production and propagation of extragalactic gamma rays, and the examination of the ultimate nature of matter and of physics beyond the standard model through searches for dark matter and the effects of quantum gravity [4] .

In the atmospheric Cherenkov technique, gamma rays are detected against the abundant background produced by hadronic showers. In order to improve the signal to noise ratio of the experiment, it is necessary to reject a significant fraction of hadronic showers. Traditional background rejection methods based on image shape parameters have been extensively used for the data from imaging telescopes. However, non-imaging Cherenkov telescopes have to develop very different means of identifying and removing cosmic ray events. Methods for the efficient discrimination of photon and hadron initiated showers have been derived from the differences in the intrinsic properties of the Cherenkov radiation from pure electromagnetic and hadronic cascades.

The parameters derived from Cherenkov images include Hillas, fractal and wavelet moments [5], while those obtained from non-image Cherenkov data consist of pulse profile rise-time and base width and the relative ultraviolet to visible light content of the Cherenkov event. It is shown by a neural-net approach that these parameters, when used in suitable combinations, can bring about a proper segregation of the two event types [6].

Among the non- imaging parameters is the lateral distribution of Cherenkov photon density which Cherenkov arrays can determine. The lateral distribution of Cherenkov light at ground level records important information on the development of the air shower which produces it. That information is important for the primary particle identification, because the shower developments at early stages strongly depend on the primary nuclei [7].

In this paper, for a big ideal array, using CORSIKA (COsmic Ray SIMulations for KAscade) code [8] existence of a hump in lateral distribution of Cherenkov photons and its dependence to energy and altitude and also its statistical fluctuations have been studied. Then in section 5, we have applied our simulation data to a Tunka-like array which is accessible from technical and economic point of view. It is shown that by using this technique in typical array, a good efficiency is achieved for gamma-hadron separation.

## 2 Monte Carlo simulation

CORSIKA code version 6.90 with the GHEISHA [9] and QGSJET [10] As low (primary momentum below 80 GeV/c) and high energy interaction models has been used to simulate Cherenkov light emission in the earth's atmosphere by the secondaries of the extensive air showers generated by proton and gamma primaries. The Cherenkov radiation produced within the specified band width (300-550 nm) is propagated to the ground. We generated more than 16,000 vertically incident air showers over the energy range from 50 GeV to 25 TeV.

In the present work, we have used CANGAROO (longitude:  $136^{\circ}47'$  E, latitude:  $31^{\circ}06'S$  and altitude: 160 m)[11], TUNKA (longitude:  $103^{\circ}04'E$ , latitude:  $51^{\circ}48'N$  and altitude: 675 m)[12] PACHMARHI (longitude:  $78^{\circ}26'E$ , latitude:  $22^{\circ}28'N$  and altitude: 1075 m)[13], ALBORZ (longitude:  $51^{\circ}6'E$ , latitude:  $35^{\circ}48'N$  and altitude: 1200 m)[14], CAT (longitude:  $1.97^{\circ}$  E, latitude:  $42.5^{\circ}$  N and altitude: 1650 m)[15] and CHACALTAYA (longitude:  $291.8^{\circ}$  E, latitude:  $16^{\circ}$  S and altitude: 5220 m) [16] as the observation levels where one big ideal Cherenkov detector in the form of a square with an area of 600m 600m is assumed. Using Geomag [17], for each observation level corresponding magnetic field is computed and used in simulation program. Using this large ideal detector, all of the emitted Cherenkov photons were used in order to build statistics. This corresponds to having an enormous detector on the ground with %100 efficiency. So, we can study ideally the lateral distribution of Cherenkov photon density.

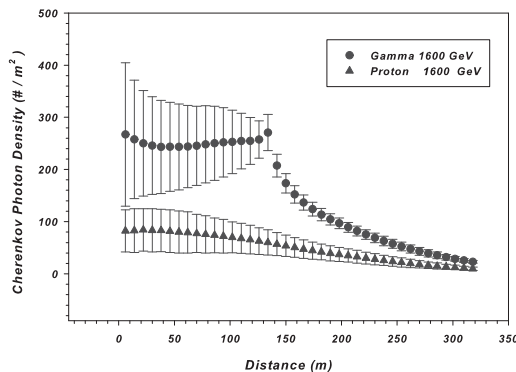


Figure 1: Lateral distribution of Cherenkov photon density and related standard deviations in TUNKA observation level (675m) averaged over 300 showers for  $\gamma$ -ray (circle) and proton (star) primaries of 1600 GeV energy.

### 3 Lateral distribution of Cherenkov photon density

The lateral distribution of Cherenkov light is observable and can be studied theoretically, as well. Although it is difficult to measure this observable phenomenon in the existing experiments, it is well within the present levels of technology and funding. It can be measured with an elaborate experimental set-up with a large number of properly spaced detectors, similar to the dedicated PeV gamma-ray experiments currently operating or being planned [18]. The fact that if this observable has the experimental potential for gamma-hadron separation is the matter of this work.

The Cherenkov lateral distribution, averaged over 300 showers, for 100 GeV gamma and 100 GeV proton primaries, is shown in Fig. 1 for TUNKA observation level (675 m). As seen, the lateral distribution shows the characteristic hump at about 134 m from the core for gamma primary. Indeed hump is present in all of the studied gamma ray-initiated showers, with different energies. So, it seems that the existence of a hump can be used as a gamma-hadron separation technique for rejecting hadronic background in gamma ray astronomy.

Origin of the hump is described as follows: High-energy electrons, once created, lose energy continuously as they travel down in the atmosphere, mainly by the bremsstrahlung process, thereby increasing their cumulative RMS scattering angle ( $\theta_s \sim 1/E$ ) or equivalently ( $\theta_s \sim e^x$ ) and emitting Cherenkov radiation all the time until they fall below the Cherenkov threshold (here  $\theta_s, E$  and  $x$  are cumulative RMS scattering angle, energy and depth of the electrons respectively). The Cherenkov angle ( $\theta_c$ ) also increases as the particle travels down since the atmospheric density and hence the refractive index increase with depth, but this increase is much slower ( $\theta_c \sim \sqrt{x}$ ) compared with  $e^x$  for scattering). There is a certain energy and depth above which the cumulative RMS scattering angle is less than the Cherenkov angle at that depth and, in this region, the emitted photons arrive at a distance nearly equal to  $h\theta_c$ , where  $h$  is the height of the production of Cherenkov photons, whereas the photons emitted by the lower-energy electrons spread out. If the contribution to the density of photons at that distance from these high-energy electrons is comparable to or larger than that due to lower-energy electrons, a hump will appear at that distance [18].

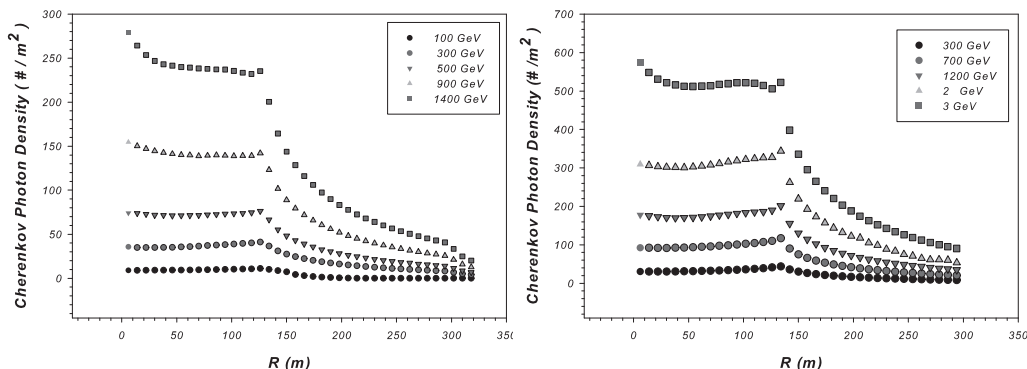


Figure 2: Lateral distribution of cherenkov photon density for  $\gamma$ -ray showers as a function of energy for TUNKA (right) and ALBORZ (left) observation levels.

## 4 Results for the ideal detector

### 4.1 Potential for gamma-hadron separation

in Fig. 1, each data point is the mean value with the corresponding standard deviation. We have applied 2m steps for distance calculations. This will provide an accuracy for determining the hump place equal to 2m. However, to avoid confusion in figure, only 8m interval, are presented. It is seen that place of hump is located at 134m from shower core for gamma initiated shower and as expected, there is not such a hump for proton primary. Also these results show good separation between gamma and proton primaries; especially there is very good separation around the hump place.

### 4.2 Hump characteristics

Different parameters can be effective in the intensity and place of hump. Among these are type of cathodes which used in detectors, earth magnetic field, coefficient of transmission(or absorption) of atmosphere [19], telescope effective collection area, fluctuation in the distribution and detection efficiency [20], primary energy of gamma shower and altitude of observation level. In the next subsections, dependence of hump characteristics to energy and altitude, and also statistical fluctuations in lateral distribution of Cherenkov photons are discussed.

#### 4.2.1 Primary Energy of gamma ray

Since it is due to higher energy electron hump is expected to be, the present even at higher primary energies; though with decreasing prominence as the shower maximum approaches the observation level. This is because, as the shower maximum approaches the observation level with increasing primary energy, the contribution from lower altitudes, where the product  $h\theta_c$ , starts decreasing becomes appreciable. In Fig. 2, we have shown the lateral distributions of gamma rays in wide energy range 50GeV-3TeV for TUNKA and ALBORZ observation levels. It is seen in this figure that hump is present up to the highest energy, though with decreasing prominence. With increasing energy, contribution of all distances become important and hump disappears at a certain energy. For TUNKA level, this energy

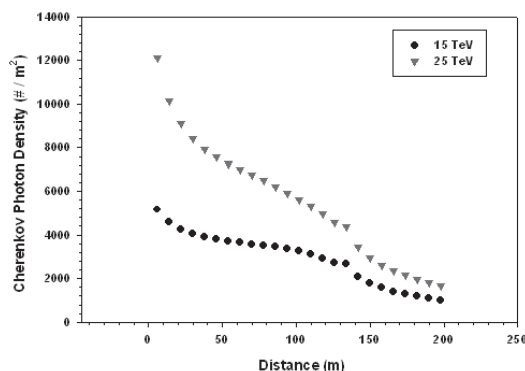


Figure 3: Lateral distribution of cherenkov photon density for TUNKA level. There is a weak hump at 15 TeV energy (circle). But at 25 TeV energy it is disappeared .

is around 25 TeV (Fig. 3). Thus, it seems that hump is present over the entire energy range where the atmospheric Cherenkov technique is used for gamma-ray astronomy.

#### 4.2.2 Hump at different altitudes

It seems that, with increasing altitude, hump place shifts toward the shower core and its prominence decreases. These are because as the altitude of observation increases, the shower maximum for a given primary energy comes closer to the observation level and the situation becomes similar to the case of a fixed observation level but with increasing primary energy [18]. Thus, we expect the hump to be present but with its prominence decreasing with altitude. In addition, because hump is placed at  $r = h\theta_c$ , the core distance at which the hump appears ( $r$ ) becomes smaller with increasing altitude, as the height to the maximum and hence the height of production of Cherenkov photons ( $h$ ) decreases. Fig. 4. Shows variation of hump place with altitude. As it seen at higher altitude, hump distance relative to shower core linearly decreases with altitude and there is a good linear fit to simulation data. With further increasing in altitude the hump disappears. This feature can be clearly seen in Fig. 5 which Shows lateral distribution of cherenkov photon density for gamma rays in CHACALTAYA observatory (5220m a.s.l). The hump completely disappears at this depth of 540 g/cm<sup>2</sup> at 1000 GeV energy as at this altitude, the contribution from higher-energy electrons closer to the observation level, becomes appreciable at near distances. Instead in this high altitude, hump exists at lower energy where the fluctuations mainly for gamma primaries are at minimum and the energy threshold is very low. As the primary gamma-ray energy increases, the altitude at which the hump disappears decreases . Thus the hump can be seen at mountain altitudes, except at very high altitudes and not too high primary energies.

#### 4.2.3 Statistical fluctuation

In Fig. 6, standard deviation per mean for Cherenkov photon density as a function of distance is shown for vertically incident gamma-ray showers of energy 1400 GeV in three different observatories. There is a common feature in all of these altitudes; fluctuations decrease with increasing distance . Specially, we have minimum fluctuations at hump. Note that, this low variance is related to the place of highest density number of Cherenkov photons namely hump (Fig. 1). So, it points to a very low fluctuation in this place and this is important

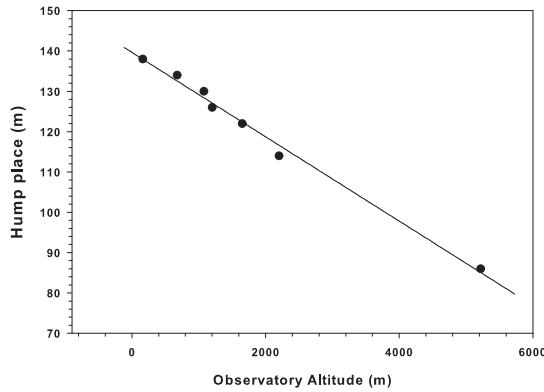


Figure 4: Hump place as a function of altitude.

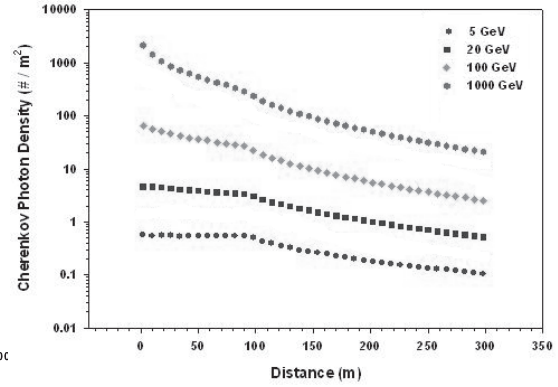


Figure 5: Lateral distribution for Chacaltaya observatory (5220 m.a.s.l)

because we use hump characteristic for gamma-hadron separation and this low fluctuation makes it very suitable for this purpose, but low fluctuation in far distance is due to small photon densities.

Relative variance as a function of energy, exactly at hump place, is represented in Fig. 7 for TUNKA, ALBORZ and PACHMARH observatories. Symbols in this graph are simulation data and lines are fitted curves. Again, we see that fluctuations are decreased with increasing energy. Also, it is clearly seen that among these three observatories, TUNKA has minimum fluctuations at hump place.

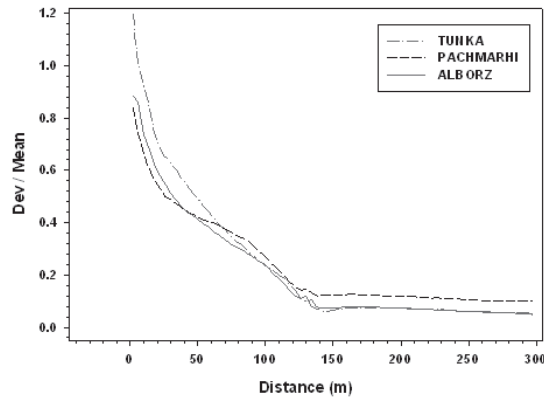


Figure 6: Relative variance as a function of distance for 1400 GeV gamma initiated showers in three different observatories.

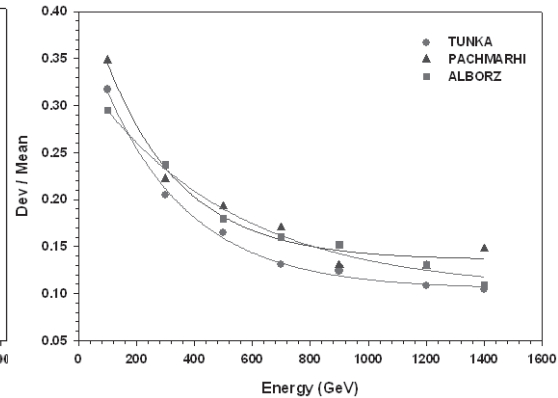


Figure 7: Relative variance profile as function of energy at hump place for three observatories.

## 5 Results for a TUNK- like array

As we know, efficiency of detection and segregation of cosmic rays improves with increasing number of detectors and effective collective area. Hump characteristics are discussed in

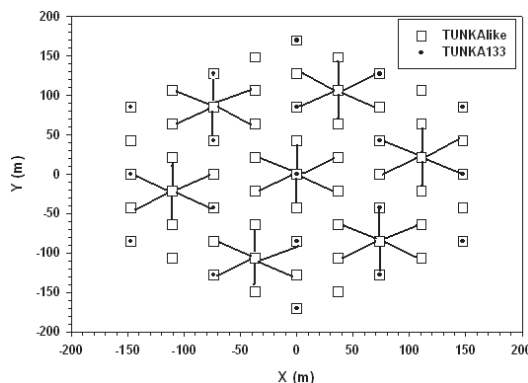


Figure 8: TUNKAlike array. Minimal distance between detectors is 42.5 m. Seven detectors form a cluster. Filled circles show position of TUNKA-133 detectors. (only detectors in  $r \leq 170$  m distance are shown.)

previous sections for an ideal array. But in practice, economic and technical conditions cause to use limited collective area and number of detectors in current experiments. These results in large statistical fluctuations, hence decrease the accuracy of energy and mass determination.

To investigate real potential of hump characteristic for gamma-hadron separation we apply this technique to a TUNKA-like array which has the same shape and arrangement as TUNKA133 array. The Tunka-133 EAS Cherenkov array (longitude:103° 04'E, latitude: 51° 48'N , and altitude: 675 m)[12] consists of 133 optical detectors which are grouped into 19 clusters with seven detectors in each one (six hexagonally arranged detectors and one in the center)[22]. An optical detector consists of a metallic cylinder of 50 cm diameter .The distance between the detectors is 85 m.

To decrease fluctuations, we have suggested a TUNKA-like array with 1m diameter detectors and 42.5cm separation, i.e. increasing the area of optical detector by a factor of 4 and decreasing separation by a factor of half. Shape and arrangement of TUNKA-133 array is kept unchanged in this TUNKA-like array. Then, vertically incident air showers with fixed core position at the centre of the array are simulated for proton and gamma ray primaries in this TUNKA-like array. Since hump is placed at 134m from shower axis at TUNKA observation level (section 4.2.2), detectors far to 170m are enough to study hump characteristics. Plan of the TUNKA-like array is shown in Fig. 8

Lateral distribution of Cherenkov light for showers from gamma rays in wide energy range  $10^{-2}$ TeV-10TeV for TUNKA-like array and in TUNKA observation levels are presented in Fig. 9. Again, this array shows hump up to the highest energy but with decreasing prominence.

Lateral distributions of Cherenkov photon density of 1600 GeV  $\gamma$ -ray and proton primaries are obtained for this TUNKA-like and presented in Fig. 10. Each data point in this figure is the mean value of 300 showers with the corresponding standard deviation. Again gamma and proton are separated and we have good separation, specially around hump place. We expects hump at 134 m from shower core (Fig. 4), but in this TUNKA-like array we do not have instated detector in this place. We see a peak at 127m detector . Also as expected there is not such a hump for proton primary.

To find hump place exactly and compare its place with ideal array, we have fitted the lateral distribution data:  $Q(r)$  in TUNKA-like array with  $Q(r) = Q_0 + a * e^{br}$  (for  $r \leq 0$

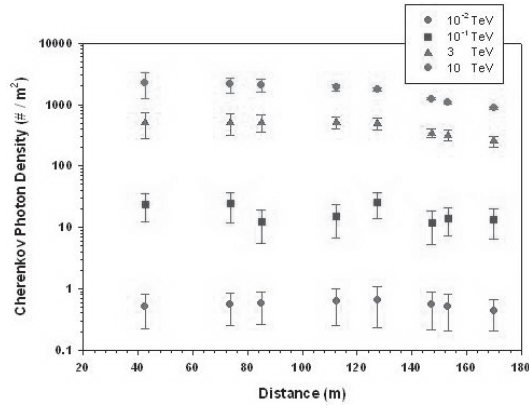


Figure 9: Lateral distribution of Cherenkov photon density and related standard deviations in TUNKA-like array averaged over 300 showers for  $\gamma$ -ray primaries of  $10^{-2}$  TeV -10 TeV energy ranges.

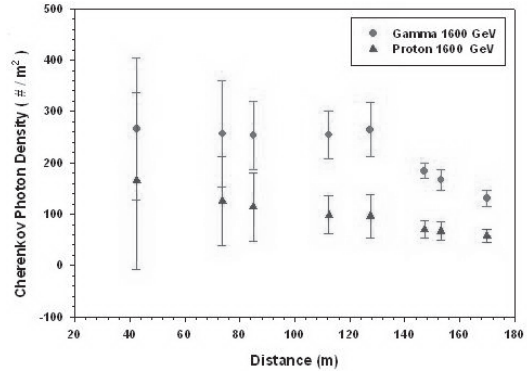


Figure 10: Lateral distribution of Cherenkov photon density and related standard deviations in TUNKA-like array averaged over 300 showers for  $\gamma$ -ray (circle) and proton (triangle) primaries of 1600 GeV energy.

$\leq 127$  m) and  $Q(r) = c/(1 + d * r)$  (for  $r > 127$  m) curves. So intersection point of this two curves is hump place. Lateral distribution and related fitted curves are shown in Fig. 11 for different energies. Using this method, results for hump place and corresponding errors are summarized in table.1.

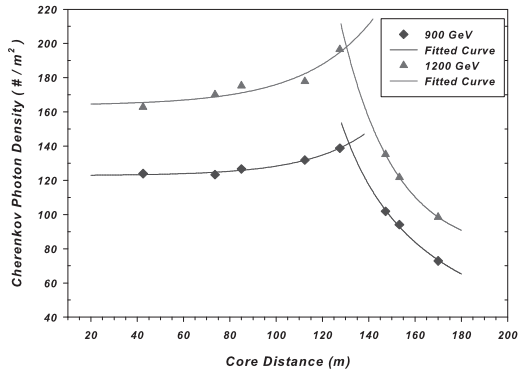


Figure 11: Lateral distribution of Cherenkov photon density in TUNKA-like array (points) and related fitted curves (lines) for 900 and 1200 GeV gamma ray primaries.

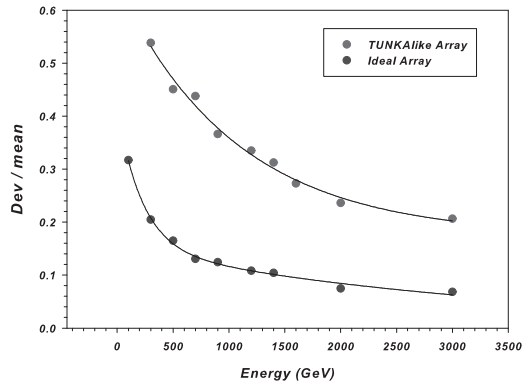


Figure 12: Standard deviation per mean at hump place in TUNKA-like and ideal array (points) with related fitted curves (lines) for gamma ray primaries at different energies.

In order to compare statistical fluctuation between ideal and TUNKA-like arrays, relative standard deviations (standard deviation per mean) are calculated at hump place in different energies and are shown in Fig. 12. It can be seen that fluctuations decrease with



Table 1: Values of hump place for TUNKA-like array in different energies.

Energy(GeV)	500	700	900	1200	1400	2000
Hump place(m)	131.7	130.0	131.1	130.3	134.3	130.2
Relative Error(%)	1.70	2.98	2.16	2.76	0.22	2.8

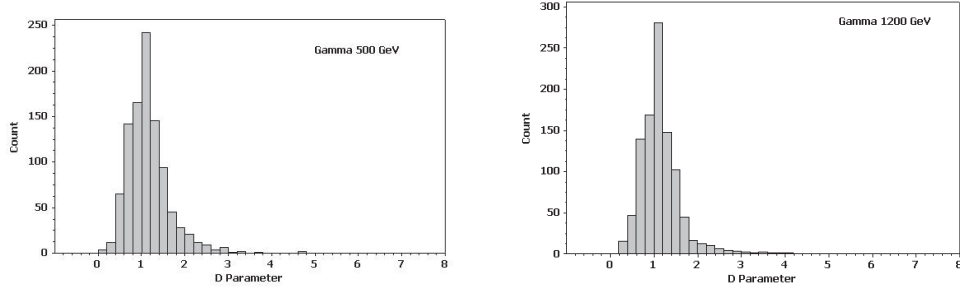


Figure 13: Distribution of D parameter for gamma primaries at 500 and 1200 GeV

increasing energy in both, ideal and TUNKA-like arrays and as expected ideal array has less fluctuations. It is interesting to note that two curves have best fit with same equation:  $y = ae^{-bx} + ce^{-dx}$ . Here x and y refer to energy and (Dev / mean) respectively.

### 5.1 Hump potential for single shower separation

As mentioned in previous sections all derived values for lateral distribution was mean of 300 simulated showers. To investigate potential of hump characteristic for separation a single gamma induced shower from a hadron one, we introduce a separation parameter D, which is defined as  $D = \frac{Q_{127}}{Q_{112}}$  where  $Q_{127}$  and  $Q_{112}$  are Cherenkov photon density at 127m and 112m distance from shower core respectively. By considering Fig. 10, we conclude that,  $D > 1$  and  $D < 1$  are related to a gamma and proton primary respectively. Distributions of D parameter for 1000 simulated gamma primaries in 500 and 1200 Gev are presented in Fig. 13. In this graphs, we see that about %63 of 1200 GeV and %62 of 500 Gev gamma induced showers have  $D > 1$ . Also, these distributions for proton primary are presented

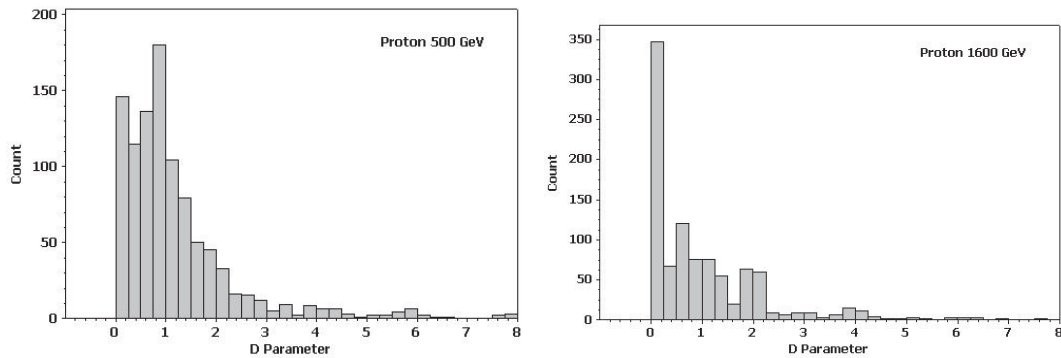


Figure 14: Distribution of D parameter for proton primaries at 500 and 1600 GeV

in Fig. 14. Here %61 of 1600 GeV protons and %58 of 500 GeV protons have,  $D < 1$ . Distributions of D parameter for gamma and proton in 100 GeV are presented in Fig. 15. It is seen that we have very good separation between gamma and proton primaries.

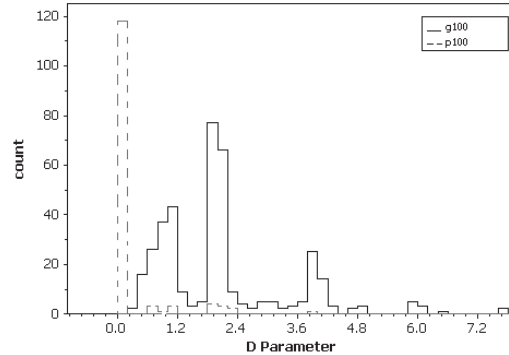


Figure 15: Distributions of D parameter for gamma and proton in 100 GeV.

## 6 Results

Using CORSIKA code, the existence of a hump in lateral distribution of Cherenkov photon in gamma induced showers and its different characteristics are studied. We have shown hump prominence and its place can be affected by energy of gamma ray primary and altitude of observatory, respectively. Moreover, by considering a TUNKA-like array, actual potential of typical available arrays to use this technique for gamma-hadron separation is discussed. We have obtained %63 efficiency for 1200 GeV gamma primaries. In the evaluation of efficiency of this method, reciprocal effect of energy and altitude must be considered simultaneously. It is true that increasing of energy results to more efficiency for detection of Cherenkov photons for both gamma and proton primaries, but as mentioned in the text, for each altitude, hump exists up to a certain energy which by increasing energy above that, a weak hump appears in lateral distribution of Cherenkov photon density and consequently efficiency of this method decreases. Note that this certain energy decreases with increasing altitude so that, at higher altitude observatories, hump appears in lower energy where the fluctuations mainly for gamma primaries are at minimum and the energy threshold is very low, at the limit 20 GeV and where the density of Cherenkov light for proton shower is very low. So, it could be useful tool also for future potential experiments at high altitude laboratories and at lower energies.

## References

- [1] Arqueros F. et al., 2002 , *Astropart.Phys.*, 17 , 3, 293-318
- [2] Andringa S. et al., 2007, *Proc. 30th ICRC* , Mexico, 3 1321
- [3] Ohm S. et al., 2009, *Astropart.Phys.*, 31, 5, 383-391
- [4] CTA consortium.eprint, 2010, arXiv1008.3703c
- [5] Hillas A., 1996, *Space Science Review*, 75, 17

- [6] Razdan A. et al., 2002, *Astropart.Phys.*, 17, 4, 497-508
- [7] Tokuno H. et al., 2003, *Proc. 28th ICRC*, Japan, 17, 497
- [8] Heck D. et al., 1998, *Forschungszentrum Karlsruhe Report FZKA*, 6019
- [9] Heck D. and Engel R., 2003, *Proc. 28th ICRC*, Japan, 7, 279
- [10] Kalmykov N. N. et al., 1997, *Nucl. Phys. B (Proc. Suppl.)*, 52B, 17
- [11] Nishijima K. et al., 2005, *Proc. 29th ICRC*, Pune, 5, 327
- [12] Budnev N. M. et al., 2005, *Proc. 29th ICRC*, Pune, 8, 255
- [13] Majumdar P. et al., 2003, *Astroparticle Physics*, 18, 333
- [14] <http://sina.sharif.edu/> -observatory
- [15] Barrau A. et al., 1998, *NIMPA.*, 416, 2-3, 278-292
- [16] Saavedra O. and Jones L. W., 2001, *NCimC.*, 024, 497
- [17] <http://www.ngdc.noaa.gov/seg/geomag/magfield.shtml>
- [18] Rao M.V.S. and Sinha S., 1988, *J. Phys. G: Nucl. Phys.*, 14, 811
- [19] Patterson J.R. and Hillas A.M., 1983, *J.Phys. G:Nucl Phys.*, 9, 1433
- [20] Portocarrero C. E. and Arqueros F., 1998, *J.Phys. G:Nucl Part. Phys*, 24, 235
- [21] Rahman M. A. et al., 2001, *ExA.*, 11, 113
- [22] Prosin V.V et al., 2009, *NuPhS.*, 190, 247